JAMI
Journal of Applied Mathematics and Informatics
J. Appl. Math. & Informatics Vol. **42***(2024), No. 4, pp. 931 - 943*
https://doi.org/10.14317/jami.2024.931

THE ELEVATION OF EFFICACY IDENTIFYING PITUITARY TISSUE ABNORMALITIES WITHIN BRAIN IMAGES BY EMPLOYING MEMORY CONTRAST LEARNING TECHNIQUES

S. SINDHU*, N. VIJAYALAKSHMI

Abstract. Accurately identifying brain tumors is crucial for medical imaging's precise diagnosis and treatment planning. This study presents a novel approach that uses cutting-edge image processing techniques to automatically segment brain tumors. with the use of the Pyramid Network algorithm. This technique accurately and robustly delineates tumor borders in MRI images. Our strategy incorporates special algorithms that efficiently address problems such as tumor heterogeneity and size and shape fluctuations. An assessment using the RESECT Dataset confirms the validity and reliability of the method and yields promising results in terms of accuracy and computing efficiency. This method has a great deal of promise to help physicians accurately identify tumors and assess the efficacy of treatments, which could lead to higher standards of care in the field of neuro-oncology.

AMS Mathematics Subject Classification : 65H05, 65F10.
Key words and phrases : Image processing, pyramid network algorithm, automatic segmentation.

1. Introduction

Medical image processing is a field of study and application within medical imaging that focuses on the development and implementation of techniques and algorithms to analyze and manipulate images generated from various medical imaging modalities. These modalities include X-rays, computed tomography (CT), magnetic resonance imaging (MRI), ultrasound, and more. locating key structures or areas of interest in the medical imaging and highlighting them. As in the case of separating malignancies from nearby healthy tissue in an MRI

Received December 14, 2023. Revised February 27, 2024. Accepted March 14, 2024.
*Corresponding author.

scan. According to the National Health Organization's data study on tumor survey, in 2040, there would be about 25000 new cases of cancer and about 28000 persons [1] with brain tumor cells. The annual increase in brain tumor cases is over 2%. Due to early medical researchers, children today are also impacted by brain tumors. According to the WHO report, around 3% of deaths were gradually increasing year by year. This kind of death rate increases because of the later detection of infected areas and their size and level of infection in the body organs. The tissues that were formed in the brain may be cancer or a tumor. Every tissue will not be cancerous. There are two types of tumors [2]: malignant and benign. The malignant tumor cells will increase in shape and size in a particular area and also spread the infection to other body organs too. If organs will not work properly, then only people will go to the hospital and visit the manual inspections. The benign is another type of tumor cell in the brain; it will increase in shape and size but infect other body organs. Early stage identification helps treat the patient in the right way and at the right time to save their life. In the proposed work to concentrate the segmentation of the infected area even in different sizes and levels of infection using memory contrast learning technique [3]. Fragmenting and dividing the video material into frames is the fundamental task for the identification and analysis of the video. The model is supplied a frame at a time for image segmentation. Even at the microscopic level, the image segmentation makes it simple to identify the diseased area by its size and form.

Scope of the 3D-Model MRI Brian image segmentation

Locating key structures or areas of interest in the medical imaging and highlighting them. As in the case of separating malignancies from nearby healthy tissue in an MRI scan [4]. With a variety of neurological diseases, the three-dimensional magnetic image of the brain is segmented to identify the disease. The segmented image is used by the radiologist to determine the dimensions, position, and form of an infected area, assisting in the prompt treatment of the patients. For patients to receive the best care, exact or perfect image segmentation is crucial. It makes it possible to create individualized treatment programs that are based on each patient's particular brain structure, enhancing treatment results and minimizing adverse effects. A critical step in medical image analysis is 3D MRI segmentation, which opens the door to cutting-edge methods including lesion quantification, texture analysis, and feature extraction. Clinical practice, research, and the creation of cutting-edge healthcare solutions are all significantly impacted by the crucial and dynamic field of 3D MRI brain image segmentation [5]. It is essential for expanding our knowledge of brain illnesses and for providing patients with improved therapy [6].

Drawback of the medical image segmentation in resection

The quality of segmentation can vary depending on factors including image quality, noise, and the algorithm utilized, and image segmentation techniques may not always deliver perfect accuracy. The accuracy of surgical planning and execution may be impacted by these errors. There are times when sampling is insufficient to find all types of tumor cells in the brain [7]. Synthetic picture synthesis can be used to solve problems of this nature. To train the model to forecast the outcome with a more accurate score, increase the sampling.

2. Related works

In recent years, brain tumor detection and segmentation have been the focus of numerous studies aiming to enhance diagnosis and treatment. One notable study published in 2023 introduced a novel approach towards multi-modal anatomical landmark detection for ultrasound-guided brain tumor resection. The researchers employed contrastive learning, CNN MLP, and 3D SIFT algorithms to detect landmarks, contributing to more precise surgical procedures. Their work, indexed in SCI, utilized the RESECT dataset, leading to the development of a 3D model and a specialized loss function, emphasizing targeted regression error. However, the study also identified a gap in inter-modal landmark identifications, suggesting an avenue for future research to explore further integration of different imaging modalities for enhanced detection accuracy. In a different vein, a study from 2020 investigated the potential of hyperspectral imaging (HIS) for detecting brain tumor pixels and their malignant phenotypes. This research, indexed in IEEE, sought to utilize non-invasive imaging techniques to classify tumors. By analyzing hyperspectral images, the researchers aimed to identify malignant phenotypes and boundaries of glioblastomas. Although promising, this approach raises questions regarding its applicability in clinical settings and the need for further validation studies to ensure its reliability and accuracy. Another significant contribution comes from a 2022 paper focusing on the segmentation of brain tumor objects in MRI images using the Connected Component Labeling (CCL) algorithm. This study, indexed in SCI, employed morphological operations such as closing to segment tumor objects accurately. Utilizing the BraTS2022 dataset, the researchers demonstrated effective segmentation of meningiomas, highlighting the importance of precise segmentation for treatment planning and monitoring. However, the study primarily addressed the segmentation of specific-sized objects, leaving room for exploration in handling various tumor sizes and shapes encountered in clinical practice. Additionally, a study from 2020 investigated the performance of image thresholding techniques, particularly the Otsu technique, for brain tumor segmentation. Published in Scopus, this research evaluated the Watershed algorithm using BraTS2018 and BraTS2019 datasets. By analyzing thresholding methods, the study aimed to enhance edge detection and region segmentation in MRI images. However, challenges remain in determining optimal thresholds, emphasizing the need for robust techniques to address variations in image quality and tumor characteristics. Furthermore, an earlier study from 2019 proposed the development of automated brain tumor identification using MRI images. Indexed in IEEE Explorer, the study utilized the OTSU algorithm on a brain tumor dataset from figshare. While the study achieved comparative tumor detection, questions arise regarding its reliability in real-world clinical settings and its comparability with expert radiologists' assessments. Lastly, a study from 2017 explored brain tumor detection based on segmentation using MATLAB. Published in Scopus, this research employed various edge detection and segmentation algorithms, including Sobel, Prewitt, and Canny, along with K-means clustering and CNNs like VGG-16. Despite achieving promising results, the study highlighted computational challenges, including increased processing time and memory requirements, underscoring the importance of optimizing algorithms for practical implementation.

3. Proposed Methods

In this proposed work, to elucidate the novel approach algorithm called Segmenting Object by Learning Pyramid Network (SOLPN). In this algorithm first calculate the image from the video scenario and it could be find the image inflectional region area detection and classifications. It is really good at identifying and categorizing important areas in these pictures [**?**, **?**, **?**, **?**, **?**, **?**, **?**, **?**]. The fundamental power of SOLPN is its capacity to identify critical areas in the visual data extracted from videos. It efficiently detects important sections in video frames by navigating through their complexity using a pyramid network [**?**, **?**] design. Interestingly, SOLPN does this by using sophisticated learning strategies and taking advantage of the hierarchical structure that visual information naturally possesses.

3.1. Dataset. The online repository has a variety of image sets, including V7, BraTS, Kaggle, UCI Learn, MedImage, and others. T1W, T2W, and FlAIR pictures are the three forms of magnetic image resonance images used in the suggested technique. Comparatively, the suggested effort is most closely related to the 3D-based FLAIR pictures. Even at the microscopic level, these images aid in the tissue detection process.

Table 1. Displays the FLAIR image's contrasting hues as captured by the MRI.

Tissues	FLAIR image
CSF	Dark color representation
FAT	Lighter than inflammation background
Inflammation	Little brighter from background
Echo timing	114

Because of the aforementioned difficulty, only the proposed study employs the FLAIR-based MRI 3D modal dataset to accurately forecast the form of tumor tissues in the brain, even when those tissues have abnormally shaped and sized tissues.

The RESECT dataset is more suited for the segmentation and analysis of video in the proposed work. Twelve gigabytes of MRI scanner photos and video

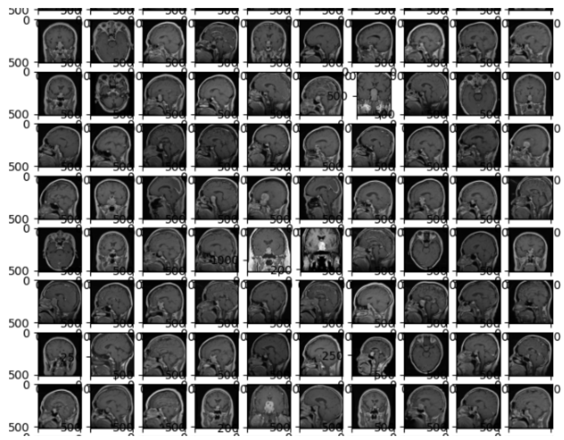

FIGURE 1. RESECT brain tissue dataset

are included in this dataset. The suggested work to increase the effectiveness of image segmentation to recognize the tissues generated in the human brain performs better thanks to the original scanned images.

These comprised 1458 non-cancerous pictures, 1687 gliomas, 1457 pituitary tumors, and 1538 malignant tissues. Every picture was extracted from the video scanning data, with each frame being recognized and given as a distinct image. When compared to all other prior techniques, the suggested work to concentrate various types of tissue in the brain has been found to produce greater results.

4. Implementation of the proposed method

The dataset from the previous study, Augment-based optimum spanning soloV3 method, could be fed into the current work. Let's investigate whether the algorithm can identify any more tissues in the brain nerves or tumors. The memory contrast-based approach is used in this proposed study to enhance the segmentation process's efficiency in brain picture processing.

The memory contrast-based approach usually works at the color contrast level of each pixel value. A specific type of contrastive learning employed in deep learning, memory-contrast, or MoCo for short, is particularly useful for creating powerful image representations. Each model in the memory bank had its negatives, or images that were different from one another. The quality of detection is enhanced because of the model's initialization, which determines which cells are not tumor cells. This may enhance the tumor's or infected cell's accuracy within the neuronal circuits of the brain. This memory bank helps the model recognize distinguishing features by offering a more diverse set of negative samples for training.

The Momentum Encoder Traditionally, contrastive learning uses two distinct encoders (networks) to create queries and keys. In MoCo, a single encoder known as the "query encoder" generates queries for positive pairs. The "momentum encoder," a moving average of the query encoder's parameters, generates keys. This creates a kind of temporal uniformity that enhances learning stability.

The pyramid scene parsing network algorithm is frequently employed to segment photos based on their semantic content. This approach, which is frequently suggested for segmenting images from videos or recordings, may build a basic network for regional elucidation analysis. As a result, the instance image segmentations may perform better.

It could use the subsequent approach to segment instantly by following the stages.

Step 1: Module for image pooling. At this point, the picture can be recognized, and a convolutional network can be built based on its many stages. The Pyramid Pooling Module, which is utilized to gather context information from various spatial scales, is the most unique feature of SOLO-PSN. The input feature map is divided into areas of varying sizes by this module, which then extracts global context data from each region. Then, by fusing these context elements, a more detailed and comprehensive understanding of the scene is captured. The scenario is given in Figure 2.

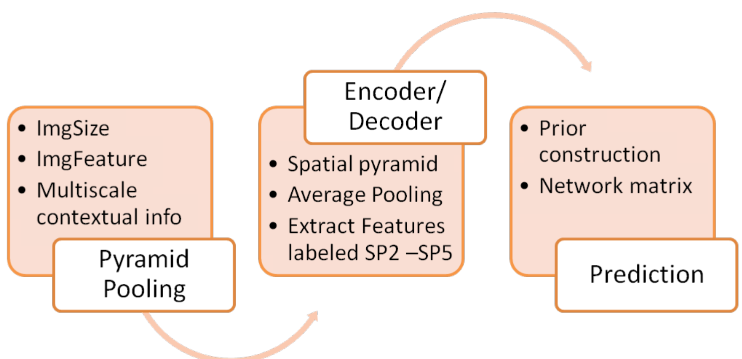

Figure 2. Using encoder and decoder in pyramid pooling for feature extraction.

The input image (Img) is transformed into a grayscale image, and the color contrast is adjusted to prevent problems with color contrast during regional detection. Conceptually, the image splits into $S \times S$ uniform grids. The task of developing the model to determine the semantic category and semantic object of an image instance falls on each grid cell. Using its dimensional output, which represents the likelihood of classes in a semantic image, each grid in the semantic category predicts the Number of Classes (C). The output's space will be $S \times S \times C$ once the image has been converted to $S \times S$ grids.

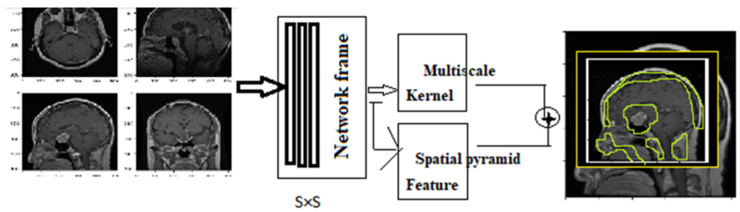

FIGURE 3. Semantic network fragment for feature extraction.

Figure 3 illustrates the presumption that every grid cell pertains to a single image instance, hence solely falling under the semantic category. The decoupled SOLO method will be used in this proposed work in conjunction with the Pyramid network model for classification and prediction.

The encoder-decoder architecture used by PSPNet is described as follows. While the decoder portion sharpens the segmentation output, the encoder portion is in charge of extracting features from the input image and producing feature maps.

Dilated Convolutions: To enhance the receptive field without downsampling the feature map and preserve fine-grained features in the segmentation outcome, PSPNet employs atrous (dilated) convolutions in the encoder network.

ResNet Backbone: PSPNet frequently uses a ResNet as its backbone network, usually utilizing the well-known CNN architectures ResNet-50 or ResNet-101. Strong feature extraction capabilities are offered by this.

Typically, RestNet employs numerous layers to determine error rates and generates neural detection layers ranging from 20 to 56 layers. It results in a gradient value of an increased error rate from zero. first mapping, let the network adjust,

$H(x) = F(x) + x$ is the result of $F(x) := H(x) - x$ Here, x is an identity, and $F(x)$ and $H(x)$ denotes the weight layers. Segmenting instances within the grid cell (i, j) is the responsibility of the k-th channel, where $k = i \cdot S + j$ (i and j indexed starting from zero). Consequently, a clear relationship is shown between semantic categories and class-agnostic masks. It produces excellent segmentation results and does a great job of gathering rich context information.

5. Memory contrast learning with pyramid network and SOLOV3

The memory contrast learning algorithm is the suggested technique for the work that is being offered. It has the potential to be executed by creating an eight-layer pyramid network and connecting it to the SOLOV3 algorithm from earlier work. Although supervised datasets are frequently used in memory contrast learning, the suggested approach begins with an image that is converted to grayscale and generates binary data for accessing each individual pixel in order to develop each network layer with the desired characteristics. It entails comparing samples from a memory bank that are positive and samples that are negative. The model learns to distinguish between samples that are similar and those that are not by using the memory bank, which acts as a storehouse of information from historical data. This method is mostly applied to learning tasks that are semi-supervised or self-supervised.

The general process of memory contrast learning is as follows:

- Memorandum Bank: Organize features or embeddings taken from historical data into a memory bank.
- Pairs, Positive and Negative: Choose a set of positive and negative pairs to work with during training.
- Train the model to minimize a contrastive loss function.
- Momentum encoders, or Siamese networks: Siamese networks process the positive and negative samples using two identical subnetworks.
- Online Aggregation: To maintain a fixed capacity, online aggregation of the memory bank is carried out.
- Memory Maintenance: Methods for choosing or balancing the representations that are kept in the memory bank are also used.

Level 1. Add the picture to a network frame for pyramid pooling. At this point, the model could be loaded with the picture dimensions, features, and multiscale contextual data for training.

Level 2. The features of the image could be recovered at this level from the raw data image scenario that the scanner equipment stores. The scanning device typically saves the image as a video. A frameset has been retrieved from the video picture. Based on the metrics, each frameset could then be fed into the frame set segmentation procedure.

Level 3: Pyramid Pooling Network. This stage will involve creating an image network. It can represent the features obtained from multi-scale contrast-based data at various spatial pyramid scalings.

Table 2. Features categorization

Type	Measures	Features
Intensity-Based Features	Voxel intensity	Mean, skewness, kurtosis, histogram-based features, and texture features derived from intensity variations.
Texture-Based Features	spatial patterns	co-occurrence matrices (e.g., Haralick features), run-length matrices
Edge and Boundary Features	Structures	edge strength, density, smoothness, wavelet-based features

TABLE 3. Encoder and decoder model

Datasets	Resource	Model	Mean IoU	Pixel Acc
RESECT brain tissue dataset	8 GPUs	PSPNet50 (Baseline)	0.7802	0.9513
	8 GPUs	PSPNet50 (Our)	0.7644	0.9400
	8 GPUs	PSPNet50 (Our + Skip(Out1))	0.77414	0.9431
	8 GPUs	PSPNet50 (Our + Skip(Out1, Stem))	0.78141	0.9501
	1 GPU	PSPNet50 (Our)	0.7378	0.9322
	8 GPUs	PSPNet101 (Baseline)	0.7963	0.9550
	8 GPUs	PSPNet101 (Our)	0.7931	0.9487

Level 3: Limitations discovered. At this stage, the model recognizes the retrieved features and applies the wavelet approach to the threshold finding procedure.

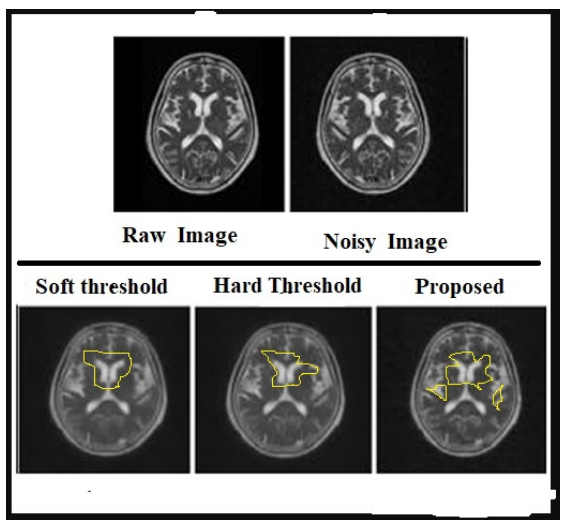

FIGURE 4. The outcome of Proposed threshold compared with other methods

TABLE 4. Mean square error and Peak_signal_noise_ratio

MSE	0.01	0.03	0.05	0.1	PSNR	0.01	0.03	0.06	0.1
Hard threshold	310	603	643	1,4,95	Hard threshold	23.21	20.33	20.06	16.49
Soft threshold	388	785	771	1,627	Soft threshold	22.64	19.29	19.26	16.01
Proposed	147	311	341	625	Proposed	26.46	23.20	23.20	20.17

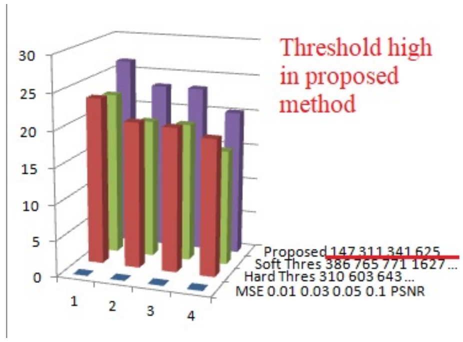

Figure 5. Graphical representation of the proposed method high in co-efficient value

It frequently denotes the benefits, qualities, or distinctive features that make the suggested approach stand out. It can suggest that this approach is more accurate, efficient, or effective than earlier ones at producing the intended result.

6. Result and Analysis

The evaluation metrics for the brain pituitary image are as follows: Metrics based on F-measures, such as:

- Intersection-over-Union (IoU) and Dice Similarity Coefficient (DSC),
- Specificity (Spec) and Sensitivity (Sens),
- The Rand Index (Acc) and Accuracy,
- The area under the ROC curve (AUC),
- Receiver Operating characteristic (ROC).

All that the f-measures are is an F-score, which is a standard statistic for determining how well the suggested model performs for computer vision techniques. This overlap between the segmentation and ground value can be computed using the sensitivity and prediction precision values. It comprises aspects that are strongly required by medical pictures and precision with false positive values. Table 5 shows the F-Score for the proposed algorithms.

Table 5. F-Score for the proposed algorithms

F-Score (IoU & DSC)	Accuracy Score False Positive	Accuracy Score False Negative
0.01	0.03	0.04
0.04	0.04	0.05
0.04	0.001	0.056

Table 6 illustrates that the suggested approach has a lower F-score than alternative methodologies, resulting in superior accuracy, where accuracy and dependability of the results are crucial. They indicate that your models or techniques are exhibiting remarkable performance in identifying patterns, forecasting, or accurately classifying data.

Table 6. Comparison of F-Scores

Metrics	Proposed Approach vs. Alternative Approaches
Accuracy Score	Higher
Dependability	Higher

7. Conclusions

The important importance that accurate brain tumor delineation plays in efficient medical imaging diagnosis and treatment planning is highlighted by the study's result. The novel approach that is being given, which makes use of sophisticated image processing methods, particularly Pyramid with SOLOv3 Algorithm, demonstrates strong and accurate tumor boundary delineation in MRI scans. Especially, the combination of several algorithms effectively addresses problems related to tumor heterogeneity and different forms and sizes. Reliability of the method is consistently validated by evaluations conducted on RESECT Dataset, which show excellent results in terms of accuracy and computational efficiency denoted by F-Score. As it can assist physicians in accurate tumor identification and treatment assessment, this method has the potential to raise the bar for neuro-oncology care and is a major step in the right direction for better patient outcomes.

Conflicts of interest : This declaration makes it abundantly evident that none of the project's writers have any financial, professional, or personal interests that could affect the study's findings or conclusions. Even though there are no disputes, the statement's presence emphasizes.

Data availability : Not applicable

Acknowledgments : Grateful for the invaluable advice and criticism that Dr. N. Vijayalakshmi, an assistant professor at the SRM Institute of Science and Technology (Sr. G), provided during the course of this study.

References

1. H. Kasban, M.A.M. El-Bendary, & D.H. Salama, *A comparative study of medical imaging techniques*, International Journal of Information Science and Intelligent System **4** (2015), 37-58.
2. A. Mohan, D. Rastogi, & K. Rajput, *3D U-NET Convolutional Neural Network for Segmentation of Brain Tumour Tissues in Hgg and Lgg Magnetic Resonance Imaging*, In 2022 6th International Conference On Computing, Communication, Control And Automation (ICCUBEA), August 2022, pp. 1-4, IEEE.

3. R. Tamilselvi, A. Nagaraj, M.P. Beham, & M.B. Sandhiya, *Bramsit: A database for brain tumor diagnosis and detection*, In 2020 Sixth International Conference on Bio Signals, Images, and Instrumentation (ICBSII), February 2020, pp. 1-5, IEEE.
4. V. Sravan, K. Swaraja, K. Meenakshi, P. Kora, & M. Samson, *Magnetic resonance images based brain tumor segmentation-a critical survey*, In 2020 4th international conference on trends in electronics and informatics (ICOEI), June 2020, pp. 1063-1068, IEEE.
5. A. Mustaqeem, A. Javed, & T. Fatima, *An Efficient Brain Tumor Detection Algorithm Using Watershed & Thresholding Based Segmentation*, IJIGSP, **4** (2012), 34-39. DOI: 10.5815/ijigsp.2012.10.05
6. K.N. Guy-Fernand, J. Zhao, F.M. Sabuni, & J. Wang, *Classification of brain tumor leveraging goal-driven visual attention with the support of transfer learning*, In 2020 Information Communication Technologies Conference (ICTC), May 2020, pp. 328-332, IEEE.
7. J.L. Foo, *A survey of user interaction and automation in medical image segmentation methods*, Tech rep ISUHCI20062, Human Computer Interaction Department, Iowa State Univ., 2006.
8. M. Havaei, H. Larochelle, P. Poulin, & P.M. Jadoin, *Within-brain classification for brain tumour segmentation*, Int. J. Cars **11** (2016), 777–788.
9. D. Müller, I. Soto-Rey, & F. Kramer, *Towards a guideline for evaluation metrics in medical image segmentation*, BMC Res Notes **15** (2022), 210. https://doi.org/10.1186/s13104-022-06096-y
10. H. Zhao, J. Shi, X. Qi, X. Wang, & J. Jia, *Pyramid scene parsing network*, In Proceedings of the IEEE conference on computer vision and pattern recognition, 2017, pp. 2881-2890.
11. H. Fang, & F. Lafarge, *Pyramid scene parsing network in 3D: Improving semantic segmentation of point clouds with multi-scale contextual information*, Isprs journal of photogrammetry and remote sensing **154** (2019), 246-258.
12. S. Chen, Y. Song, J. Su, Y. Fang, L. Shen, Z. Mi, & B. Su, *Segmentation of field grape bunches via an improved pyramid scene parsing network*, International journal of agricultural and biological engineering **14** (2021), 185-194.
13. Z. Zhang, S. Gao, & Z. Huang, *An automatic glioma segmentation system using a multilevel attention pyramid scene parsing network*, Current Medical Imaging **17** (2021), 751-761.
14. X. Wang, R. Zhang, C. Shen, T. Kong, & L. Li, *Solo: A simple framework for instance segmentation*, IEEE transactions on pattern analysis and machine intelligence **44** (2021), 8587-8601.
15. S. Salari, A. Rasoulian, H. Rivaz, & Y. Xiao, *Towards multi-modal anatomical landmark detection for ultrasound-guided brain tumor resection with contrastive learning*, In International Conference on Medical Image Computing and Computer-Assisted Intervention, October 2023, pp. 668-678, Cham: Springer Nature Switzerland.
16. H. Zhu, Q. Yao, L. Xiao, & S.K. Zhou, *You only learn once: Universal anatomical landmark detection*, in Medical Image Computing and Computer Assisted Intervention–MICCAI 2021: 24th International Conference, Strasbourg, France, September 27–October 1, 2021, Proceedings, Part V 24. Springer, 2021, pp. 85–95.
17. A. Tripathi, M.R. Panicker, A.R. Hareendranathan, J. Jaremko, Y.T. Chen, K.V. Narayan, & C. Kesavadas, *Unsupervised landmark detection and classification of lung infection using transporter neural networks*, Computers in Biology and Medicine **152** (2023), 106345.
18. Y. Xiao, M. Fortin, G. Unsgård, H. Rivaz, & I. Reinertsen, *Retrospective evaluation of cerebral tumors (RESECT): A clinical database of pre-operative MRI and intra-operative ultrasound in low-grade glioma surgeries*, Medical Physics **44** (2017), 3875–3882.
19. B. Rister, M.A. Horowitz, & D.L. Rubin, *Volumetric image registration from invariant keypoints*, IEEE Transactions on Image Processing **26** (2017), 4900–4910.
20. K. You, S. Lee, K. Jo, E. Park, T. Kooi, & H. Nam, *Intra-class Contrastive Learning Improves Computer Aided Diagnosis of Breast Cancer in Mammography*, in Medical Image

Computing and Computer Assisted Intervention–MICCAI 2022: 25th International Conference, Singapore, September 18–22, 2022, Proceedings, Part III. Springer, 2022, pp. 55–64.
21. L.-H. Cheng, X. Sun, & R.J. van der Geest, *Contrastive Learning for Echocardiographic View Integration*, in Medical Image Computing and Computer Assisted Intervention–MICCAI 2022: 25th International Conference, Singapore, September 18–22, 2022, Proceedings, Part IV. Springer, 2022, pp. 340–349.
22. X. Liu, E.R. Bonner, Z. Jiang, H.R. Roth, S.M. Anwar, R.J. Packer, et al., *Automatic segmentation of rare pediatric brain tumors using knowledge transfer from adult data*, In 2023 IEEE 20th International Symposium on Biomedical Imaging (ISBI), April 2023, pp. 1-4, IEEE.
23. M.W. Wagner, et al., *Radiomic features based on MRI predict progression-free survival in pediatric diffuse midline glioma/diffuse intrinsic pontine glioma*, Can Assoc Radiol J. 2022, 8465371221109921.
24. J.L. Leach, et al., *MR imaging features of diffuse intrinsic pontine glioma and relationship to overall survival: report from the International DIPG Registry*, Neuro Oncol **22** (2020), 1647-1657.
25. U. Baid, et al., *The RSNA-ASNR-MICCAI BraTS 2021 Benchmark on Brain Tumor Segmentation and Radiogenomic Classification*, arXiv:2107.02314, 2021.
26. A. Myronenko, *3D MRI brain tumor segmentation using autoencoder regularization*, International MICCAI Brainlesion Workshop, Springer, Cham, 2018.
27. F. Isensee, P.F. Jaeger, S.A. Kohl, J. Petersen, & K.H. Maier-Hein, *nnU-Net: a self-configuring method for deep learning-based biomedical image segmentation*, Nature Methods (2020), 1-9.
28. R. Madhogarhia, et al., *Automated segmentation of pediatric brain tumors based on multiparametric MRI and deep learning*, SPIE Medical Imaging **12033** (2022), 120332R.
29. J. Ker, Y. Bai, H.Y. Lee, J. Rao, & L.P. Wang, *Automated brain histology classification using machine learning*, Journal of Clinical Neuroscience **66** (2019), 239–245.
30. S.S. Yadav & S.M. Jadhav, *Deep convolutional neural network based medical image classification for disease diagnosis*, J. Big Data **6** (2019), 113.
31. J. Ker, S.P. Singh, Y. Bai, J. Rao, T. Lim, & L.P. Wang, *Image Thresholding Improves 3-Dimensional Convolutional Neural Network Diagnosis of Different Acute Brain Hemorrhages on Computed Tomography Scans*, Sensors **19** (2019), 2167.
32. J. Ker, L.P. Wang, J. Rao, & T. Lim, *Deep Learning Applications in Medical Image Analysis*, IEEE Access **6** (2018), 9375-9389.

S. Sindhu working as Assistant Professor. Department of Computer Science and pplications, SRMIST, Ramapuram, Chennai, India. She is also a research scholar at SRMIST, Ramapuram, Chennai. His research interests include numerical optimization and biological computation.

Department of Computer Science and Applications, SRM Institute of Science and Technology, Ramapuram, Chennai.
`e-mail: sindhus1@srmist.edu.in`

N. Vijayalakshmi, working as Assistant Professor in the department of Comptuer Science and application at SRMIST, Ramapuram, Chennai, India.

Department of Computer Science and Applications, SRM Institute of Science and Technology, Ramapuram, Chennai.
`e-mail: vijayaln@srmist.edu.in`